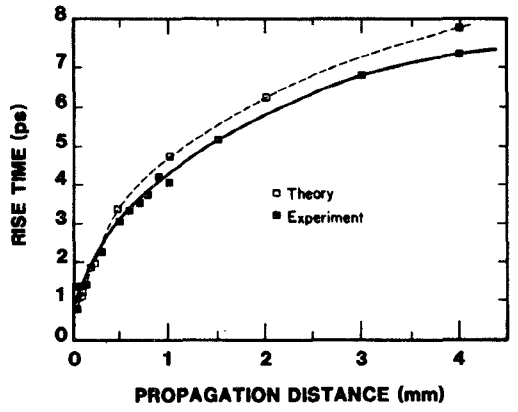

Fig. 7. Rise time of distorted pulse as a function of propagation distance. Theoretical values are compared against those experimentally measured (Courtesy: K. Meyer, University of Rochester, NY).

both cases. This implies that ultrashort pulses (having bandwidths greater than 700 GHz for this case) will suffer greater dispersion in the coplanar line. On the other hand, since the increase of ϵ_{eff} with frequency begins more gradually for coplanar lines, longer pulses with narrow bandwidth experience less variation of ϵ_{eff} and hence less distortion. This difference of behavior is illustrated in Fig. 4. The dispersion of both coplanar and microstrip lines can be reduced by reducing the substrate thickness. For coplanar lines, dispersion can also be slightly reduced by decreasing the strip and slot dimensions, but the ϵ_{eff} at low frequency remains lower then the corresponding microstrip and thus it is intrinsically more dispersive for short pulses.

The only experimental measurement of dispersion in coplanar transmission lines, to our knowledge, has been made at the University of Rochester [9], [10] on lithium tantalate substrates using an electrooptic sampling technique. Consequently, calculations were made for their experimental configuration which utilizes two coplanar strips each 50 μ wide and separated by 50 μ on a 500-μ thick $LiTaO_3$ substrate having $\epsilon_r = 43$. The numerically derived dispersion curve is shown in Fig. 5. For this case, the constants in curve-fitting (17) are $\epsilon_q = 23.68$, $a = 51.3$, $b = 1.69$, and $f_{\text{TE}} = 23.15$ GHz. Using their experimentally measured pulse shape at 0.9 mm (Fig. 6(a)) with the falling edge extrapolated (the data supplied was truncated), the pulse shape at 4 mm was computed (Fig 6(b)) from the dispersion relation. The agreement with the experimental result (Fig. 6(c)) is found to be reasonable. The frequency dependence of the characteristic impedence and that of the losses in the conductor and substrate is expected to have very little effect on the pulse distortion in coplanar lines, extrapolating from the calculations made for the microstrip line in our previous paper [3]. Pulse dispersion was also calculated for different distances of propagation and 10–90 percent risetime plotted as a function of distance. Again good agreement with experimental data supplied is obtained (Fig. 7).

IV. Conclusions

A computer program has been developed to generate dispersion relations for coplanar-type transmission lines up to terahertz frequencies for a wide range of configurations and dimensions. The number of terms in the field expansions and the order of the gaussian quadrature integration are specified in order to optimize computing time. A simple approximate formula also has been presented which can give dispersion relations for coplanar waveguides for a wide range of parameters. The results have been used to predict distortion of picosecond electrical pulses propagating in such lines. Good agreement has been obtained with available experimental results on $LiTaO_3$ substrates.

Dispersion of coplanar waveguides has been compared to an equivalent microstrip (same substrate thickness and characteristic impedance) and is found to be more for subpicosecond pulses but less for longer pulses. Finally, we note that dispersion in coplanar lines can be greatly reduced by using a superstrate of the same material, which would remove the inhomogeneity of the medium.

Acknowledgment

The authors wish to thank K. Meyer and Prof. G. Mourou for sharing their experimental results, and Profs. T. Itoh and C. Schwartz for helpful discussions.

References

[1] C. H. Lee, *Picosecond Optoelectronic Devices*.. New York: Academic Press, 1984.
[2] K. C. Gupta, R. Garg, and I. J. Bahl, *Microstrip Lines and Slotlines*. New York: Artech House, 1979.
[3] G. Hasnain, G. Arjavalingam, A. Dienes, and J. R. Whinnery, "Dispersion of picosecond pulses on microstrip transmission lines," *SPIE Proc.* vol. 439, pp. 159–163, Aug. 1983.
[4] K. K. Li, G. Arjavalingam, A. Dienes, and J. R. Whinnery, "Propagation of picosecond pulses on microwave striplines," *IEEE Trans. Microwave Theory Tech.*, vol. MTT-30, pp. 1270–1273, 1982.
[5] T. Itoh, and R. Mittra, "Dispersion characteristics of slot lines," *Electron Lett.*, vol. 7, pp. 364–365, July 1971.
[6] J. B. Knorr and K. D. Kuchler, "Analysis of coupled slots and coplanar strips on dielectric substrate," *IEEE Trans. Microwave Theory Tech.*, vol. MTT-23, pp. 541–548, July 1975.
[7] D. S. Jones, *The Theory of Electromagnetism*. New York: Pergamon, 1964.
[8] E. Yamashita, K. Atsuki, and T. Ueda, "An approximate dispersion formula of microstrip lines for computer aided design of microwave-integrated circuits," *IEEE Trans. Microwave Theory Tech.*, vol. MTT-27, pp. 1036–1038, 1979.
[9] G. Mourou and K. E. Meyer, "Subpicosecond electrooptic sampling using coplanar strip transmission lines," *Appl. Phys. Lett.* vol. 45, no. 5, pp. 492–494, Sept. 1984.
[10] K. E. Meyer and G. Mourou, private communication.

Birefringence Analysis of Anisotropic Optical Fibers Using Variational Reaction Theory

RUEY-BEEI WU AND CHUN HSIUNG CHEN

Abstract—**The variational reaction theory is applied to achieve a variational equation for the study of the single-mode optical fibers with anisotropic core media. Emphasized in this paper are the numerical results for the birefringence of the two principal modes in discussing the effects due to differences in refractive indices, anisotropy parameters, and index profiles.**

I. Introduction

Optical fibers have found applications in various areas due to the properties of low loss, high performance, electromagnetic immunity, and small size. Recently, single-mode optical fibers have received great attention because of small dispersion, but the fundamental HE_{11} modes in two orthogonal polarizations are

Manuscript received September 23, 1985; revised January 8, 1986. This work was supported in part by the National Science Council, Republic of China, under Grant NSC 74-0608-E002-02.

The authors are with the Department of Electrical Engineering, National Taiwan University, Taipei, Taiwan, Republic of China.

IEEE Log Number 8607981.

degenerate due to the circular symmetry in fibers. Hence, a small perturbation or an imperfection in the ambient conditions may make the polarization of a mode statistically varying as it is propagated along the fibers [1].

To counteract this effect, elliptical core/cladding deformation and stress anisotropy [2]–[6] have been introduced to result in the highly birefringent fibers that can transmit single polarized waves for a long distance. These polarization-maintaining fibers are useful in coherent communication systems [7], fiber-optical sensors [8], and are compatible with integrated optical circuits [9].

In characterizing the birefringent optical fibers, it is important to calculate the birefringence, the difference between the propagation constants, of the two orthogonal HE_{11} modes. Various methods have been devoted to the analysis of isotropic-optical fibers with noncircular geometry or inhomogeneous material, such as the perturbation approximation [10], circular-harmonic computer analysis [11], finite-element method [12]–[14], and finite-difference method [15]. However, there still lacks a rigorous method for the analysis of anisotropic-optical fibers. A variational method has been employed for homogeneous and transversely anisotropic fibers [16], but is uneasy for more general cases where inhomogeneity or even arbitrary anisotropy is encountered.

Recently, a variational reaction theory [17] has been established to treat the scattering and propagation problems associated with dielectric structures. This theory is characterized by achieving a variational formulation that may properly absorb the radiation and continuity conditions and then employing the finite-element method together with the frontal solution technique to solve the variational equation. This theory can be easily extended to arbitrarily-shaped guiding structures involving inhomogeneous and even anisotropic materials. In this paper, we investigate the birefringence characteristics of the anisotropic optical fibers with various index differences, anisotropy parameters, and index profiles.

II. Variational Formulation

Optical fibers for guidance of electromagnetic waves have become essential parts of optical systems. Unlike the traditional metal-walled waveguides commonly adopted in microwave systems, there is no clear distinction between the "interior" and "exterior" regions in optical fibers. Both regions are merged into each other so that not only the scattered wave but also the guided wave may be excited by an arbitrarily incident wave. This thus provides a motivation of considering the scattering problem of a uniform optical fiber illuminated by an obliquely incident plane wave.

Let the fiber be arbitrary in shape and consist of inhomogeneous and anisotropic materials. The permeability is a scalar μ; while the permittivity tensor $\bar{\bar{\epsilon}}$ is

$$\bar{\bar{\epsilon}} = \begin{bmatrix} \epsilon_{xx} & \epsilon_{xy} & \epsilon_{xz} \\ \epsilon_{yx} & \epsilon_{yy} & \epsilon_{yz} \\ \epsilon_{zx} & \epsilon_{zy} & \epsilon_{zz} \end{bmatrix} = \begin{bmatrix} \bar{\bar{\epsilon}}_{tt} & \bar{\epsilon}_{tz} \\ \bar{\epsilon}_{zt}^T & \epsilon_{zz} \end{bmatrix} \tag{1}$$

where the subscript t means the component transverse to the z direction, and the superscript T means the transpose of a matrix.

For the scattering problem, we can assume that the incident plane wave $(\bar{E}^i, \bar{H}^i)$ and thus the scattered wave $(\bar{E}^s, \bar{H}^s)$ have the common phase factor $e^{j(\omega t - \beta z)}$. Hence, this phase factor is omitted throughout this paper so that the problem can be reduced to a two-dimensional one.

Based on the variational reaction theory [17], we choose an artificial boundary with radius r_o, outside which is a homogeneous region with material constant (ϵ_o, μ_o). The scattered field in the outside region can be expanded by the Hankel's functions, i.e.,

$$\begin{bmatrix} E_z^s \\ \eta_o H_z^s \end{bmatrix} = \sum_{m=-\infty}^{\infty} \begin{bmatrix} e_m^s \\ h_m^s \end{bmatrix} H_m^{(2)}(k_t r)\, e^{jm\phi}, \qquad r > r_o \tag{2}$$

where $k_t = \sqrt{k_o^2 - \beta^2}$, $k_o = \omega\sqrt{\mu_o \epsilon_o} = 2\pi/\lambda_o$, $\eta_o = \sqrt{\mu_o/\epsilon_o}$, (r, ϕ) is the polar coordinate and e_m^s, h_m^s are the scattering coefficients.

By imposing continuity conditions along the artificial boundary, we can obtain a variational equation for the field inside the boundary, that is [17]

$$\delta I = 0$$

$$I = \int_\Omega d\Omega \begin{bmatrix} E_z^a \\ H_z^a \\ \nabla_t E_z^a \\ \nabla_t H_z^a \end{bmatrix}^T \cdot \begin{bmatrix} j\omega\left(\omega^2\mu\bar{\epsilon}_{zt}^T \bar{\bar{K}} \bar{\epsilon}_{tz} - \epsilon_{zz}\right) & 0 & -\omega\beta\bar{\epsilon}_{zt}^T \bar{\bar{K}} & \omega^2\mu\bar{\epsilon}_{zt}^T \bar{\bar{K}} \times \hat{z} \\ 0 & j\omega\mu & 0 & 0 \\ \omega\beta\bar{\bar{K}}\bar{\epsilon}_{tz} & 0 & j\omega\bar{\bar{K}}\bar{\bar{\epsilon}}_{tt} & -j\beta\bar{\bar{K}} \times \hat{z} \\ -\omega^2\mu\hat{z} \times \bar{\bar{K}}\bar{\epsilon}_{tz} & 0 & -j\beta\hat{z} \times \bar{\bar{K}} & -j\omega\mu\bar{\bar{K}} \end{bmatrix} \cdot \begin{bmatrix} E_z \\ H_z \\ \nabla_t E_z \\ \nabla_t H_z \end{bmatrix}$$

$$- \frac{1}{2\pi k_t^2} \sum_{m=-\infty}^{\infty} \int_0^{2\pi} \begin{bmatrix} E_z^a \\ H_z^a \end{bmatrix}_{(r_o,\phi)}^T e^{jm\phi}\, d\phi \left\{ \begin{bmatrix} j\omega\epsilon_o Z_m^{(2)} & -m\beta \\ -m\beta & -j\omega\mu_o Z_m^{(2)} \end{bmatrix} \cdot \int_0^{2\pi} \begin{bmatrix} E_z \\ H_z \end{bmatrix}_{(r_o,\phi)} e^{-jm\phi}\, d\phi \right.$$

$$\left. + \left(Z_m^{(1)} - Z_m^{(2)}\right) \cdot \begin{bmatrix} j\omega\epsilon_o & 0 \\ 0 & -j\omega\mu_o \end{bmatrix} \int_0^{2\pi} \begin{bmatrix} E_z^i \\ H_z^i \end{bmatrix}_{(r_o,\phi)} e^{-jm\phi}\, d\phi \right\} \tag{3}$$

where

$$\nabla_t = \frac{\partial}{\partial x}\hat{x} + \frac{\partial}{\partial y}\hat{y}$$

$$\bar{\bar{K}} = \left(\omega^2\mu\bar{\bar{\epsilon}}_{tt} - \beta^2\bar{\bar{1}}\right)^{-1}$$

$$Z_m^{(1)} = k_t r_o J_m'(k_t r_o)/J_m(k_t r_o)$$

$$Z_m^{(2)} = k_t r_o H_m^{(2)\prime}(k_t r_o)/H_m^{(2)}(k_t r_o)$$

and the integration region Ω extends over the area $r \leqslant r_o$. Note that the matrix inversion in (10) of [17] is now carried out by

$$\begin{bmatrix} j\omega\bar{\bar{\epsilon}}_{tt} & j\beta\hat{z} \times \bar{\bar{1}} \\ j\beta\hat{z} \times \bar{\bar{1}} & -j\omega\mu\bar{\bar{1}} \end{bmatrix}^{-1} = \begin{bmatrix} -j\omega\mu\bar{\bar{K}} & -j\beta\bar{\bar{K}} \times \hat{z} \\ -j\beta\hat{z} \times \bar{\bar{K}} & -j\omega\hat{z} \times \bar{\bar{\epsilon}}_{tt}\bar{\bar{K}} \times \hat{z} \end{bmatrix} \tag{4}$$

where $\bar{\bar{1}}$ is a unit tensor.

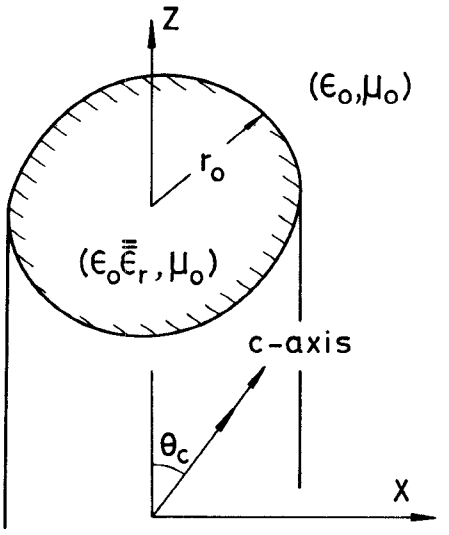

Fig. 1. Geometry of anisotropic circular fibers. $\bar{\bar{\epsilon}}_r$ is relative permittivity tensor and θ_c is angle between c-axis and z-axis.

III. Numerical Results

As shown in Fig. 1, we consider an α-power circular fiber of radius r_o with core anisotropy due to the anisotropic stress during the drawing process in manufacturing. Without loss of generality, the relative permittivity tensor of the anisotropic and inhomogeneous fiber is assumed to be

$$\bar{\bar{\epsilon}}_r = \begin{cases} \bar{\bar{1}} + \Delta \cdot \left[1-(r/r_o)^{\alpha}\right] \\ \quad \cdot \left\{ \bar{\bar{1}} + q \begin{bmatrix} \sin^2\theta_c & 0 & \sin\theta_c\cos\theta_c \\ 0 & 0 & 0 \\ \sin\theta_c\cos\theta_c & 0 & \cos^2\theta_c \end{bmatrix} \right\}, & r \le r_o \\ \bar{\bar{1}}, \quad r > r_o. \end{cases} \tag{5}$$

Here, Δ is the parameter associated with the index difference, q is the parameter to model the core anisotropy, and θ_c is the angle between the anisotropic c-axis and the z-axis. In what follows, we will investigate the effects of these parameters on the birefringence.

First, the variational equation (3) is solved by the finite-element method together with the frontal solution technique. The aim is to compute the boundary field and thus the scattering coefficients e_m^s, h_m^s for the cases with inhomogeneous waves ($|\beta| > k_o$) incident. By searching for the poles of scattering coefficients, the effective refractive index $n_e = \beta/k_o$ can be found [17]. The dispersion curves will then be given in terms of the normalized propagation constant $\mathscr{P}^2$ and the normalized frequency V where

$$\mathscr{P}^2 = (n_e^2 - 1)/\Delta$$
$$V = k_o r_o \sqrt{\Delta}. \tag{6}$$

The normalized birefringence $\Delta\mathscr{P}^2$ is thus defined as the difference between the normalized propagation constants of the two principal HE_{11}^x and HE_{11}^y modes.

Fig. 2(a) shows the propagation constants $\mathscr{P}^2$ versus the angle θ_c at frequencies $V = 1.2$, 2.1, and 3.9 for the step-index ($\alpha = \infty$) fiber with $\Delta = 0.1$, $q = 0.1$. The propagation constant of HE_{11}^x mode depends on θ_c, hence, the two principal HE_{11}^x and HE_{11}^y modes are no more degenerate as $\theta_c \neq 0°$. At the extreme case of

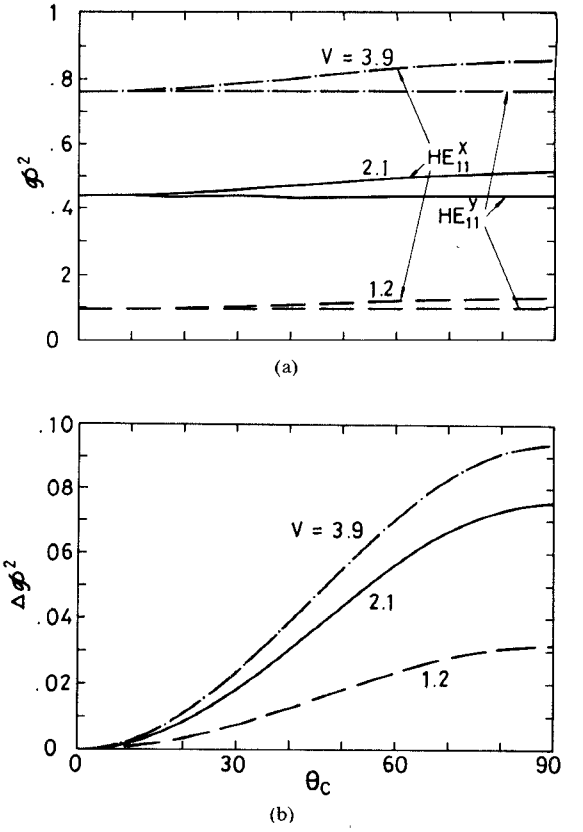

Fig. 2 Effect of c-axis angle θ_c on (a) propagation constants of and (b) normalized birefringence between principal HE_{11}^x and HE_{11}^y modes at frequencies $V = 1.2$, 2.1, and 3.9. Step-index anisotropic fiber with parameter $\Delta = 0.1$ and $q = 0.1$ is considered.

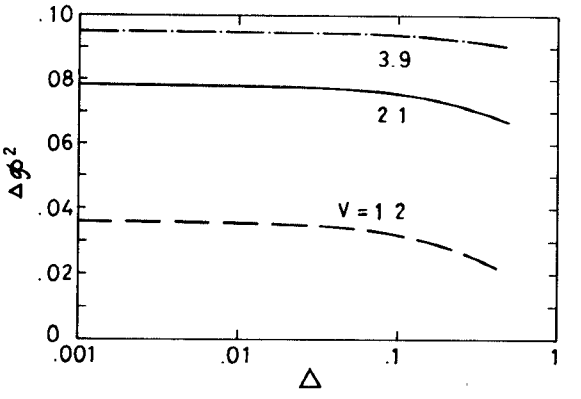

Fig. 3 Effect of index difference Δ on normalized birefringence at frequencies $V = 1.2$, 2.1, and 3.9 for step-index anisotropic fiber with $q = 0.1$ and $\theta_c = 90°$.

$\theta_c = 90°$, the anisotropy in x and y directions reaches its maximum and thus the birefringence becomes the greatest. Shown in Fig. 2(b) is the normalized birefringence $\Delta\mathscr{P}^2$ versus θ_c. It is noted that $\Delta\mathscr{P}^2$ is larger when frequency V is higher. It can be compared with the case for isotropic but elliptical fibers where the birefringence reaches its maximum and then decreases as frequency increases [10]. A further check reveals that the birefringence is proportional to $\sin^2\theta_c$, i.e., the difference between the dielectric constants in x and y directions. Therefore, only the angle $\theta_c = 90°$ is considered in the following cases.

Fig. 3 shows the effect of index difference on the normalized birefringence at frequencies $V = 1.2$, 2.1, and 3.9 for the step-

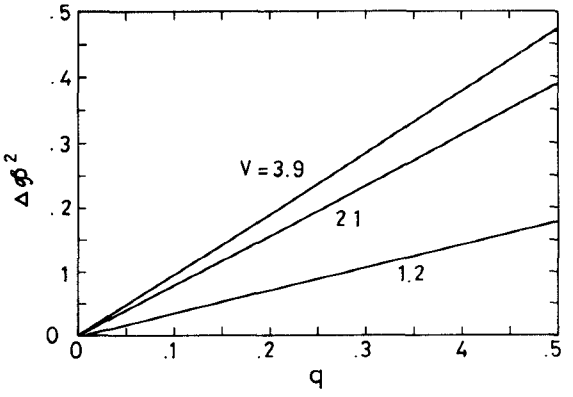

Fig. 4. Effect of anisotropy parameter q on normalized birefringence at frequencies $V = 1.2$, 2.1, and 3.9 for step-index fiber with $\Delta = 0.02$ and $\theta_c = 90°$.

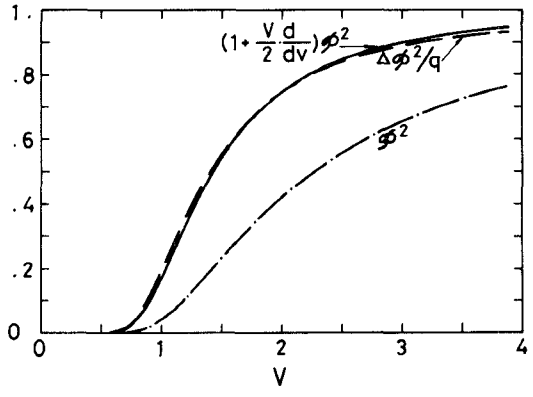

Fig. 5. Dispersion curve $\mathscr{P}^2(V)$ and birefringence curve $\Delta\mathscr{P}^2/q$ (dashed line) for step-index fiber. Solid line shows birefringence curve obtained from (8).

index fiber with $q = 0.1$. The most worthy to be stated is that the normalized birefringence $\Delta\mathscr{P}^2$ is nearly constant for $\Delta < 0.1$. It means that the birefringence $\Delta n_e = \Delta\beta/k_o$ is proportional to Δ. Since the birefringence due to core deformation is proportional to Δ^2, the core anisotropy plays a much more significant role in birefringence characteristics for the fibers with vanishing index differences.

Fig. 4 shows the effect of anisotropy parameter q at frequencies $V = 1.2$, 2.1, and 3.9 for the step-index fiber with $\Delta = 0.02$. As q tends to zero, the fiber becomes isotropic and the birefringence disappears. For larger q, where the difference between dielectric constants in x and y directions is $\Delta \cdot q$, the normalized birefringence is proportional to q. In general, it is much more easier to establish a larger q than a larger Δ for optical fibers, hence, producing core anisotropy is more promising in manufacturing highly birefringent fibers.

From the aforementioned discussions, it is concluded that $\Delta\mathscr{P}^2/q$ does define a birefringence curve for anisotropic fibers. Fig. 5 shows the dispersion curve and birefringence curve (dashed line) for a step-index circular fiber. It has been pointed out that, if the dispersion curve for a step-index isotropic fiber is $\mathscr{P}^2(V)$, then that for step-index anisotropic fiber may be approximately expressed as [16]

$$\mathscr{P}^2 = A_v \cdot \mathscr{P}^2\left(\sqrt{A_v} \cdot V\right) \tag{7}$$

where $A_v = 1$ and $1 + q$ for HE_{11}^y and HE_{11}^x modes, respectively. Therefore, the birefringence curve can be obtained approximately

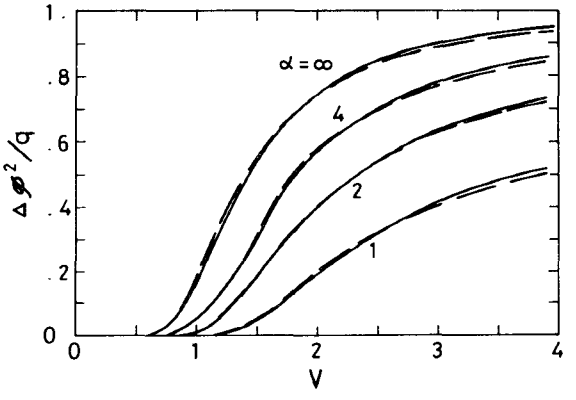

Fig. 6. Birefringence curves for α-power fibers with $\alpha = 1$, 2, 4, and infinity (step-index case). Solid and dashed lines represent results obtained from (8) and present method, respectively.

by

$$\Delta\mathscr{P}^2/q \approx \left(1 + \frac{V}{2} \cdot \frac{d}{dV}\right)\mathscr{P}^2(V). \tag{8}$$

The solid line in Fig. 5 shows the results from (8), which is compared with the dashed line with satisfaction.

Though (7) is derived for step-index fibers only, it seems also satisfactory for inhomogeneous fibers as depicted in Fig. 6, which shows the birefringence curves for α-power fibers with $\alpha = 1$, 2, 4 and infinity (step-index case). The solid lines are the results from (8), while the dashed lines are the results from our method. Since the core deformation affects little on the birefringence curve for fibers with vanishing index differences, the agreement of both results in Fig. 6 suggests that (8) may provide an efficient and accurate formula in designing even a birefringent inhomogeneous fiber.

IV. Conclusion

In this paper, the variational reaction theory and the scheme of searching for the poles of scattering coefficients have been applied to investigate the birefringence of the two principal HE_{11}^x and HE_{11}^y modes in the anisotropic fibers. For the fibers with elliptical deformation, the birefringence, which is proportional to the square of the index difference, is always very small and insignificant. On the other hand, the birefringence, due to core anisotropy, is proportional to the index difference multiplied by the anisotropy parameter and thus is much more significant. It has also been notified that the birefringence curve, which is important in describing polarization characteristics of a birefringent inhomogeneous fiber, can be approximately obtained from the dispersion curve of an isotropic circular fiber.

References

[1] F. P. Kapron, N. F. Borrell, and D. B. Keck, "Birefringence in dielectric optical waveguides," *IEEE J. Quantum Electron.*, vol. QE-8, pp. 222–225, Feb. 1972.

[2] V. Ramaswamy, W. G. French, and R. D. Standley, "Polarization characteristics on noncircular core single-mode fibers," *Appl. Opt*, vol. 17, pp. 3014–3017, Sept. 1978.

[3] V. Ramaswamy, I. P. Kaminow, and P. Kaiser, "Single polarization optical fibers: Exposed cladding technique," *Appl Phys. Lett.*, vol. 33, pp. 814–816, Nov 1978.

[4] I. P. Kaminow, "Polarization in optical fibers," *IEEE J. Quantum Electron.*, vol. QE-17, pp. 15–22, Jan. 1981.

[5] N. Imoto, N Yoshizawa, J. I. Sakai, and H. Tsuchiya, "Birefringence in single-mode optical fiber due to elliptical core deformation and stress anisotropy," *IEEE J. Quantum Electron.*, vol. QE-16, pp. 1267–1271, Nov. 1980.

[6] T. Katsuyama, H. Matsumura, and T. Suganuma, "Propagation char-

acteristics of single polarization fibers," *Appl. Opt.*, vol. 22, pp. 1748–1753, June 1983.
[7] F. Frave, L. Jeunhomme, I. Joindot, M. Monerie, and J. C. Simon, "Progress towards heterodyne-type single-mode fiber communication systems," *IEEE J. Quantum Electron.*, vol. QE-17, pp. 897–906, June 1981.
[8] S. K. Sheem and T. Giallorenzi, "Polarization effects on single-mode optical-fiber sensors," *Appl. Phys. Lett.*, vol. 35, pp. 914–917, Dec. 1979.
[9] R. A. Steinberg and T. G. Giallorenzi, "Performance limitations imposed on optical waveguide switches and modulators by polarization," *Appl. Opt.*, vol. 15, pp. 2440–2453, Oct. 1976.
[10] W. O. Schlosser, "Delay distortion in weakly guiding optical fibers due to elliptic deformation of the boundary," *Bell Syst. Tech. J.*, vol. 51, pp. 487–492, Feb. 1972.
[11] J. E. Goell, "A circular-harmonic computer analysis of rectangular dielectric waveguides," *Bell Syst. Tech. J.*, vol. 48, pp. 2133–2160, Sept. 1969.
[12] C. Yeh, K. Ha, S. B. Dong, and W. P. Brown, "Single-mode optical waveguides," *Appl. Opt.*, vol. 18, pp. 1490–1504, May 1979.
[13] N. Mabaya, P. E. Lagasse, and P. Vandenbulcke, "Finite-element analysis of optical waveguides," *IEEE Trans. Microwave Theory Tech.*, vol. MTT-29, pp. 600–605, June 1981.
[14] B. M. A. Rahman and J. B. Davies, "Finite-element analysis of optical and microwave waveguide problems," *IEEE Trans. Microwave Theory Tech.*, vol. MTT-32, pp. 20–28, Jan. 1984.
[15] E. Schweig and W. B. Bridges, "Computer analysis of dielectric waveguides: A finite-difference method," *IEEE Trans. Microwave Theory Tech.*, vol. MTT-32, pp. 531–541, May 1984.
[16] I. V. Lindell and M. I. Oksanen, "Transversely anisotropic optical fibers: Variational analysis of a nonstandard eigenproblem," *IEEE Trans. Microwave Theory Tech.*, vol. MTT-31, pp. 736–744, Sept. 1983.
[17] R. B. Wu and C. H. Chen, "On the variational reaction theory for dielectric waveguides," *IEEE Trans. Microwave Theory Tech.*, vol. MTT-33, pp 477–483, June 1985.